HHS Public Access

Author manuscript

Curr Opin Struct Biol. Author manuscript; available in PMC 2021 October 01.

Published in final edited form as:

Curr Opin Struct Biol. 2020 October ; 64: 51–58. doi:10.1016/j.sbi.2020.05.018.

Beyond Protein Structure Determination with MicroED

Chi Nguyen[1,2,3], **Tamir Gonen**[1,2,3,$]

[1]Department of Biological Chemistry, University of California Los Angeles, 615 Charles E Young Drive South, Los Angeles, CA90095

[2]Department of Physiology, University of California Los Angeles, 615 Charles E Young Drive South, Los Angeles, CA90095

[3]Howard Hughes Medical Institute, University of California Los Angeles, Los Angeles, CA90095

Abstract

Microcrystal electron diffraction (MicroED) was developed at the Janelia Research Campus as a new modality in electron cryomicroscopy (cryoEM), with the term MicroED first coined in 2013. Since then, MicroED has not only made important contributions for pushing the resolution limits of cryoEM protein structure characterization but also of peptides, small-organic and inorganic molecules, and natural-products that have resisted structure determination by other methods. This review showcases important recent developments in MicroED, highlighting the importance of the technique in fields of studies beyond protein structure determination where this MicroED is beginning to have paradigm shifting roles.

Keywords

MicroED; proteins; peptides; small-molecules; natural-products; radiation damage; crystals

Introduction

MicroED[1,2] has been pushing the limits of cryoEM in determining structures of macromolecular assemblies, peptides, and chemical compounds[1,3–5]. Prior the technological advancements in detectors[6–9] and software[10–13] that made the “cryoEM resolution

$ tgonen@g.ucla.edu.

Conflict of Interest

We wish to confirm that there are no known conflicts of interest associated with this publication and there has been no significant financial support for this work that could have influenced its outcome.

Intellectual Property

We confirm that we have given due consideration to the protection of intellectual property associated with this work and that there are no impediments to publication, including the timing of publication, with respect to intellectual property. In so doing we confirm that we have followed the regulations of our institutions concerning intellectual property.

Research Ethics

We further confirm that any aspect of the work covered in this manuscript that has involved human patients has been conducted with the ethical approval of all relevant bodies and that such approvals are acknowledged within the manuscript.

revolution[14]" possible, structure determination of biological assemblies, peptides, and chemical compounds has been dominated X-ray crystallography. To date, there are close to 150,000 depositions in the Protein Data Bank (PDB), comprised of roughly 90% X-ray, 8% NMR, and 2% EM structures. Although the first atomic resolution structure by cryoEM was already reported in 2005[15], the highest growth in TEM structure deposition has occurred in the last five years.

The field of cryoEM includes at least four major techniques: cryo-electron tomography (cryo-ET)[16,17], single-particle-analysis (SPA)[18–20], 2-dimenstional (2D) electron crystallography[21,22], and MicroED[1,2] (Figure 1). All of these cryoEM techniques exploit the advantage that electrons interact orders of magnitude more strongly with materials than X-rays, allowing the use of samples that are not tractable by other methods[23]. While CryoET and SPA use imaging, the crystallographic cryoEM methods of 2D electron crystallography and MicroED can take advantage of electron diffraction. 2D-electron crystallography is typically used for structure determination of 2D arrays, which traditionally have been of membrane proteins that are crystallized within the native environment of the lipid bilayer[22]. In contrast, MicroED uses 3D crystals and the data is collected by continuous rotation to yield structures of a wide range of samples including soluble and membrane proteins, peptides, small organic and inorganic molecules, semi-conductors, and natural-products[5,24,25,21,26]

During MicroED experiments, crystals are harvested and prepared in a number of ways for embedment on EM grids (discussed below)[1] (Figure 2). Biological samples, which are more sensitive to radiation, are typically vitrified to protect from radiation damage and to withstand the high-vacuum within the electron microscope[1,27]. Once well-diffracting crystals are detected, MicroED datasets are collected by exposure of the sample to an electron beam in diffraction mode during continuous rotation of the stage[2] (Figure 2). MicroED data are then collected on a fast camera as a movie, where each frame contains a diffraction pattern representing a wedge of the reciprocal space[27]. Because continuous rotation for MicroED is analogous to the rotation method in X-ray crystallography, the data collected can be directly processed by existing standard software such as Mosflm[28], XDS[29], DIALS[30], SHELX[31] and HKL2000[32] (Figure 2).

After data-processing, the phases are determined and structures are built using the density maps[1]. Given its wide-application and ability to extract structural information from nanocrystals, often a billionth the volume of those needed for X-ray crystallography, there are a growing number of structures determined by MicroED. Since its inception in 2013, there are close to 100 PDB entries produced by MicroED, with the highest growth in the just the past two years. To date, several laboratories have published MicroED studies and the number of practitioners is growing. Still, there are several challenges that lay ahead for MicroED including additional methodologies for sample preparation and technological developments for data collection that currently limit widespread usage of the technique. Below we discuss the most recent developments and strategies to expand the use of the MicroED.

Protein Structure Determination by MicroED

MicroED was first developed and demonstrated on proteins[1,26] and later applied to a cohort of diverse samples. Formation of large crystals continue to be the most challenging and time-consuming step for X-ray crystallography and neutron diffraction, especially for membrane proteins and protein complexes[33]. The small crystals that are typically formed by membrane proteins and protein complexes can often diffract electrons using very low exposures to minimize radiation damage (0.01 e–/Å^2)[1]. One of the earliest membrane protein structures determined by MicroED was the Ca^{2+} ATPase (PDB 3J7T/U)[34] (Figure 3A). The Ca^{2+} ATPase structure illustrated the utility of MicroED for generating Coulomb potential maps to detail information about the charged-states of amino-acid sidechains, cofactors, metals, and ligands[34]. Since Ca^{2+} ATPase, there have been several important structures determined by MicroED including the non-selective sodium-potassium (NaK) channel (PDB 6CPV)[35] and the complex of the transforming growth factor beta paired type II (TGF-βm:TβRII) (PBD 5TY4)[36] (Figure 3A–B). The MicroED structure of NaK was similar to the previously determined X-ray structure of NaK[37] but like the Coulomb maps for Ca^{2+} ATPase, the structure of NaK by MicroED allowed generation of density maps to unambiguously place Na^+ within the ion channel and to capture a new state[35]. The heterodimeric complex between TGF-βm and TβRII plays essential roles in the adaptive immune response and maintenance of the extracellular matrix[38]. Unlike Ca^{2+} ATPase and NaK, which form nanocrystals, the structure of TGF-βm:TβRII were obtained from fragmentation of large, imperfect crystals (discussed below)[36], expanding the application MicroED studies to include much larger crystals. Compared with the parent crystals, this approach led to better data by MicroED, and ultimately atomic-resolution structures[36].

MicroED in Drug Discovery

MicroED already made important contributions to drug discovery by determining structures of protein-drug complexes and supra-resolution of small-molecules and natural-products, often directly from powders without crystallization. The MicroED structure of HIV-GAG, which plays important roles in the life-cycle of HIV, was solved in complex with the antiviral drug, bevirimat (PDB 6N3U)[39] (Figure 3C). The HIV-GAG-bevirimat complex provided important information about the antiviral drug mechanism and was the first demonstration of drug discovery using MicroED, laying the foundation for its therapeutic development.

MicroED was originally intended for studying protein assemblies[1,26], however, it was rapidly recognized that this technique is a powerful tool for the characterization of small-molecules and natural-products. In 2016, the structure of the sodium channel blocker carbamezapine was determined to ~1 Å resolution[40]. In 2018, a method for small molecule sample preparation using powder to structure was described for carbamezapine[33] and later expanded to several small organic molecules[4]. In addition, the structure of MBBF4[41], a methylene blue derivative with wide medical applications including as photo-activatable antimicrobial agent[42], was also solved. Since then, several structures of small-molecules were reported by MicroED. These MicroED structures include Grippostad[41], an antiviral

drug for treatment of the common cold and the flu[43], and a recent example of the non-fulleren acceptor (NFA) semi-conductive material ITIC-Th (Figure 3D).

MicroED has also proven its usefulness for the structure determination of several natural-products that have previously been challenging or, in some cases, impossible to determine by other techniques. Unlike their synthetic small-molecules counterparts, biosynthesized natural-products are typically larger, structurally dynamic, obtained in small amounts, and are difficult to crystallize, posing considerable challenges for X-ray studies. Even when natural-products do crystallize, these crystals are often too small and are not useful for X-ray diffraction[44,45]. Brucine is an alkaloid toxin currently being tested for its anticancer properties[46] (Figure 3E). The MicroED structure of brucine at 0.9 Å resolution allowed for definitive assignment of its two chiral centers, key for understanding its toxicity and anticancer properties[4] (Figure 3). Brucine, while large compared to small-molecules, is relatively small compared to amino-acid derived natural-products called ribosomally synthesized and post-translationally modified peptides (RiPPs), including 3-thiaGlu[44] and thiostreptin[47] (Figure 3E). Glutamylated thiols, similar to the peptide modification of 3-thiaGlu, have been shown to block jasmonate and ethylene signaling pathways[48]. Thiostreptin is an antibiotic currently used in veterinary medicine[47] (Figure 3E). When efforts failed by X-ray crystallography, MicroED readily provided a 0.9 Å resolution of the 3-thiaGlu peptide (PDB 6PO6)[44]. While thiostreptin has been studied by NMR[44] and X-ray crystallography[49] previously, the ease of its characterization speaks to the robustness of MicroED for structural characterization of large, flexible natural-products (Figure 3E). Like the difficulties encountered for 3-thiaGlu, the structures of 3-substituted oxindole derivatives (Figure 3E), which contains a new stereocenter at the γ carbon installed by an enzyme through directed-evolution, was only solved with the application of MicroED[45]. These recent studies demonstrate strategies for determining the absolute configuration in small molecules based on an internal marker[44,45].

Strategies for Preparing Large Crystals for MicroED Experiments

Electrons interact much more strongly with material than X-ray[23]. This phenomenon, however, results in high absorption and, thus, electrons can only penetrate very thin materials. Thick crystals that are >500nm must be thinned before MicroED data can be collected[36]. There are two strategies for trimming large crystals to thicknesses suitable for MicroED including mechanical fragmentation (typically by sonication, vigorous pipetting, or vortexing)[36] and milling with a focused ion beam (FIB)[50–52]. Fragmentation has been successful for determining protein structures from large crystals of lysozyme, TGF-βm TβRII, xylanase, thaumatin, trypsin, proteinase K, thermolysin, and a segment of the protein tau[36]. Moving forward, the most current and promising technique for trimming large crystals for MicroED is FIB milling[50–52]. During FIB milling, a crystal is repeatedly exposed a gallium beam to trim away the surrounding materials and generate lamellas with controllable thicknesses. As proof of principle, the structure of several proteins, including lysosome and proteinase K, have been determined by FIB milling and MicroED[50–54] (Figure 4). FIB milling crystals is a relatively slow process but even then about 10 crystals can be prepared per day.

Out Running Radiation Damage and Structural Dynamics Using Fast Cameras

Radiation damage in structural studies continue to be a major challenge leading to poor processing statistics and map quality[55,56]. When electrons penetrate the sample they deposit energy and this energy deteriorates the sample, referred to as radiation damage. Radiation damage can be categorized into two forms: global and site-specific damage. Global radiation damage typically results in the disruption of the crystal lattice and can be detected during data-processing when decreases in overall diffraction intensities and increases in B-factors are observed[57,58]. On the other hand, site-specific radiation damage is not uniform, is not typically detected during data-processing, and observable only during examination of the real-space map[59]. The degree of radiation damage depends, among other things, on the content of the sample, the surrounding solution, and is proportional to the amount of energy used during diffraction studies. For MicroED, site-specific radiation damage has been illustrated to occur on specific amino-acids including cysteines, glutamate, and aspartic acids[60]. To curb the effects of radiation damage, samples are often vitrified for cryoEM studies[61]. However, even the combination of vitrification with exposure to extremely low doses of electrons (0.01 e–/Å2/s) during MicroED experiments can still lead to observable radiation damage[60].

TEMs for cryo-EM studies are typically equipped with highly-sensitive direct-electron detectors designed for optimal imaging[9,14,62]. These highly sensitive cameras, however, have not been used extensively for MicroED because of concerns of damage to the sensors. As such, MicroED data are typically collected on indirect-electron detectors such as the complementary metal oxide semiconductor (CMOS)-based CetaD and TVIPS TemCam-F416 cameras. This strategy, however, limits the availability of MicroED because most TEMs are typically outfitted with top-of-the-line direct-electron detectors and not CMOS cameras. To expand the use the TEMs, the Falcon III direct-electron camera was tested for MicroED data collection[63]. These studies demonstrate that MicroED data collected at lower electron exposure, to avoid camera damage of Falcon III, lead to greater mean completeness relative to CMOS detectors. As proof of principle, examination of maps of proteinase K from data collected on the Falcon III camera preserved the disulfide bonds (which are highly susceptible to radiation damage)[63] (Figure 5A). A similar approach was used recently with a Gatan K2 direct-electron detector in counting mode with an exposure 25 times less than for the Falcon III detector and a seemingly damage-free structure of Proteinase K has been determined.

Outrunning radiation damage using the direct electron detector Falcon III has been instrumental in determining the structures of samples that are highly susceptible to damage[44,45] and we believe that many more such examples would be forthcoming. Radiation damage was recently used to establish a pipeline for phasing MicroED data[64] (Figure 5B). A low-damage followed by a high-damage data sets were taken from the very same crystal. A difference Patterson was calculated and allowed for generation of initial phases. Following cycles of model building and refinement, the structure of a protein peptide

was determined (Figure 5B). This study demonstrates the ability to extract meaningful phase information using radiation damage in MicroED.

Concluding Remarks

MicroED is proving to be an important new tool in structural biology not only in determining structures of proteins but also of peptides, small organic and inorganic molecules, and natural-products. Continuous rotation MicroED is paradigm shifting because it has proven to be a robust, fast, and efficient method for determining the structures of small-molecules, natural-products, and semi-conductor materials without crystallization and directly from mixtures[4]. To our knowledge no other structural biology method is capable of determining atomic resolution structures directly from mixtures, making MicroED a useful and powerful tool for an array of problems that are yet to be explored. Moving forward, the application of FIB-milling and fast-cameras will certainly expand MicroED for structure determination of varying types samples with a wide-range of crystal sizes and facilitate time resolved studies. These advancements could ultimately be applied to establish automate pipelines that mirror those for X-ray crystallography to facilitate obtaining MicroED structures. Early examples of automation in MicroED has already reported in which several hundred complete data sets could be collected automatically overnight to demonstrate similar throughput as synchrotrons[65]. The application of these advancements would make MicroED more accessible for widespread use. [66,67]

Acknowledgements

We would like to thank the Gonen laboratory and all collaborators who worked with us on MicroED applications. The Gonen lab is funded by the Howard Hughes Medical Institute and the National Institutes of Health P41-GM136508.

References

*1. Shi D, Nannenga BL, ladanza MG & Gonen T Three-dimensional electron crystallography of protein microcrystals. Elife 2, 1–17 (2013).These studies mark the development and launch of MicroED from Janelia Research Campus for protein structure determination. Using lysozyme as a model system, the first MicroED structure of this protein was solved to 2.9 Å resolution.

**2. Nannenga BL, Shi D, Leslie AGW & Gonen T High-resolution structure determination by continuous-rotation data collection in MicroEDED. Nat. Methods 11, 927–930 (2014). [PubMed: 25086503] Important accompanying studies to the launch of MicroED in 2013 that illustrates continuous-rotation data collection. This work demonstrates that continuous-data collection for MicroED leads to better processing statistics, which can be achieved using already existing X-ray crystallography software.

3. Rodriguez JA et al. Structure of the toxic core of α-synuclein from invisible crystals. Nature 525, 486–490 (2015). [PubMed: 26352473]

**4. Jones CG et al. The CryoEM Method MicroED as a Powerful Tool for Small Molecule Structure Determination. ACS Cent. Sci 4, 1587–1592 (2018). [PubMed: 30555912] After the successful application of MicroED for proteins, this techniques was applied for structure detemination of small-molecules and natural-products. These studies tout a “powder to structure” pipeline where structures of small-molecules and natural-products were obtained minutes after sample prepration and MicroED data collection. Further, this work illutrates the precision of MicroED in obtaining structures from polymorphic mixtures of small-moleucles and natural-products.

*5. Nannenga BL & Gonen T The cryo-EM method microcrystal electron diffraction (MicroED). Nat. Methods 16, 369–379 (2019). [PubMed: 31040436] This review outlines the development of

MicroED form 2013-2019, highlighting important achievements that establish MicroED as an important addition to the field of cryoEM.

6. Bai XC, Fernandez IS, McMullan G & Scheres SHW Ribosome structures to near-atomic resolution from thirty thousand cryo-EM particles. Elife 2013, 2–13 (2013).
7. Herzik MA, Wu M & Lander GC Achieving better-than-3-Å resolution by single-particle cryo-EM at 200 keV. Nat. Methods 14, 1075–1078 (2017). [PubMed: 28991891]
8. Li X et al. Electron counting and beam-induced motion correction enable near-atomic-resolution single-particle cryo-EM. Nat. Methods 10, 584–590 (2013). [PubMed: 23644547]
9. Myasnikov A, Zheng S, Bulkley D, Cheng Y & Agard D K3 - A First Look at The New Direct Electron Detection Camera from Gatan Company. Microsc. Microanal 24, 890–891 (2018).
10. Wagner T et al. SPHIRE-crYOLO is a fast and accurate fully automated particle picker for cryo-EM. Commun. Biol 2, 1–13 (2019). [PubMed: 30740537]
11. Zivanov J et al. New tools for automated high-resolution cryo-EM structure determination in RELION-3. Elife 7, 1–22 (2018).
12. Tegunov D & Cramer P Real-time cryo-electron microscopy data preprocessing with Warp. Nat. Methods 16, 1146–1152 (2019). [PubMed: 31591575]
13. Punjani A, Rubinstein JL, Fleet DJ & Brubaker MA CryoSPARC: Algorithms for rapid unsupervised cryo-EM structure determination. Nat. Methods 14, 290–296 (2017). [PubMed: 28165473]
14. Kühlbrandt W The resolution revolution. Science (80-.). 343, 1443–1444 (2014).
15. Gonen T et al. Lipid-protein interactions in double-layered two-dimensional AQP0 crystals. Nature 438, 633–638 (2005). [PubMed: 16319884]
16. Komeili A, Li Z, Newman DK & Jensen GJ Magnetosomes Are Cell Membrane Invaginations Organized by the Actin-Like Protein MamK. Science (80-.). 311, 242–246 (2006).
17. Murphy GE & Jensen GJ Electron cryotomography of the E. coli pyruvate and 2-oxoglutarate dehydrogenase complexes. Structure 13, 1765–1773 (2005). [PubMed: 16338405]
18. Frank J The Cavendish Laboratory, Free School Lane, Cambridge CB2 3RQ, UK. 1, 159–162 (1975).
19. Schultz P Cryo-electron microscopy of vitrified specimens. Q. Rev. Biophys 21, 129–228 (1988). [PubMed: 3043536]
20. Taylor DW et al. Structures of the CRISPR-Cmr complex reveal mode ofRNA target positioning. Science (80-.). 348, 581–586 (2015).
21. Wisedchaisri G, Reichow SL & Gonen T Advances in structural and functional analysis of membrane proteins by electron crystallography. Structure 29, 1381–1393 (2011).
22. Henderson R et al. Model for the structure of bacteriorhodopsin based on high-resolution electron cryo-microscopy. J. Mol. Biol 213, 899–929 (1990). [PubMed: 2359127]
23. Henderson R The Potential and Limitations of Neutrons, Electrons and X-Rays for Atomic Resolution Microscopy of Unstained Biological Molecules. Q. Rev. Biophys 28, 171–193 (1995). [PubMed: 7568675]
24. Mahamid J et al. Visualizing the molecular sociology at the HeLa cell nuclear periphery. Science (80-.). 351, 969–972 (2016).
25. Wrapp D et al. Cryo-EM structure of the 2019-nCoV spike in the prefusion conformation. Science (80-.). 367, 1260–1263 (2020).
26. Nannenga BL, Shi D, Hattne J, Reyes FE & Gonen T Structure of catalase determined by MicroED. Elife 3, e03600 (2014). [PubMed: 25303172]
27. Shi D et al. The collection of microED data. Nat Protoc 11, 895–904 (2016). [PubMed: 27077331]
28. Battye TGG, Kontogiannis L, Johnson O, Powell HR & Leslie AGW iMOSFLM: A new graphical interface for diffraction-image processing with MOSFLM. Acta Crystallogr. Sect. D Biol. Crystallogr 67, 271–281 (2011). [PubMed: 21460445]
29. Kabsch W et al. XDS. Acta Crystallogr. Sect. D Biol. Crystallogr 66, 125–132 (2010). [PubMed: 20124692]
30. Waterman DG et al. Diffraction-geometry refinement in the DIALS framework. Acta Crystallogr. Sect. D Struct. Biol 72, 558–575 (2016). [PubMed: 27050135]

31. Sheldrick GM & Gould RO Structure solution by iterative peaklist optimization and tangent expansion in space group P1. Acta Crystallogr. Sect. B 51, 423–431 (1995).

32. Otwinowski Z & Minor W Processing of X-ray diffraction data collected in oscillation mode. Methods Erizymol. 276, 307–326 (1997).

33. Fromme P & Spence JCH Femtosecond nanocrystallography using X-ray lasers for membrane protein structure determination. Curr. Opin. Struct. Biol 21, 509–516 (2011). [PubMed: 21752635]

**34. Yonekura K, Kato K, Ogasawara M, Tomita M & Toyoshima C Electron crystallography of ultrathin 3D protein crystals: Atomic model with charges. Proc. Natl. Acad. Sci. U. S. A 112, 3368–3373 (2015). [PubMed: 25730881] These studies successfully launch the application of MicroED for structure determination of membrane proteins. Further, Coulomb maps generated from electron diffraction allow assignment of charges in Ca2+ ATPase.

**35. Liu S & Gonen T MicroED structure of the NaK ion channel reveals a Na+ partition process into the selectivity filter. Commun. Biol 1, 1–6 (2018). [PubMed: 29809203] These studies firmly establish the application of MicroED for structure determination of membrane proteins. Using nanocrystals, MicroED captured two new conformations of Nak and visualization of the sodium within the channel, important missing links in the study of this family of proteins.

36. De La Cruz MJ et al. Atomic-resolution structures from fragmented protein crystals with the cryoEMEM method MicroEDED. Nat. Methods 14, 399–402 (2017). [PubMed: 28192420]

37. Alam A & Jiang Y Structural analysis of ion selectivity in the NaK channel. Nat. Struct. Mol. Biol 16, 35–41 (2009). [PubMed: 19098915]

38. Morikawa M, Derynck R & Miyazono K TGF-β and the TGF-β family: Context-dependent roles in cell and tissue physiology. Cold Spring Harb. Perspect. Biol 8, (2016).

*39. Purdy MD et al. MicroED structures of HIV-1 Gag CTD-SP1 reveal binding interactions with the maturation inhibitor bevirimat. Proc. Natl. Acad. Sci. U. S. A 115, 13258–13263 (2018). [PubMed: 30530702] The structure of HIV-GAG bound the anti-viral drug bevirimat provided important insights into its mechanism of action. Using MicroED for structures determination of protein-drug complexes establishes its application for structures-based drugs design.

40. Van Genderen E et al. Ab initio structure determination of nanocrystals of organic pharmaceutical compounds by electron diffraction at room temperature using a Timepix quantum area direct electron detector. Acta Crystallogr. Sect. A Found. Adv 72, 236–242 (2016). [PubMed: 26919375]

*41. Gruene T et al. Rapid Structure Determination of Microcrystalline Molecular Compounds Using Electron Diffraction. Angew. Chemie - Int. Ed 57, 16313–16317 (2018).These studies also establish that MicroED is a powerful tool for structure determination using powders of small molecules. These studies illustrate the expanded use of MicroED in the field biology and chemistry.

42. Wainwright M Methylene blue derivatives - Suitable photoantimicrobials for blood product disinfection? Int. J. Antimicrob. Agents 16, 381–394 (2000). [PubMed: 11118846]

43. Koytchev R et al. Evaluation of the efficacy of a combined formulation (Grippostad®-C)in the therapy of symptoms of common cold: A randomized, double-blind, multicenter trial. Int. J. Clin. Pharmacol. Ther 41, 114–125 (2003). [PubMed: 12665160]

**44. Ting CP et al. Use of a scaffold peptide in the biosynthesis of amino acid-derived natural products. Science (80-.). 365, 280–284 (2019).Crystals of the natural product 3-thiaglu, a RiPP with a novel peptide modification with biological activities, failed to generate a structure by X-ray crystallography. MicroED achieved a 0.9 Å resolution of 3-thiaglu to allow asignment of the absolute configuration of its stereocenters, providing imporant insights into the mechanims for the installation of this unique modification.

**45. Dick M, Sarai NS, Martynowycz MW, Gonen T & Arnold FH Tailoring Tryptophan Synthase TrpB for Selective Quaternary Carbon Bond Formation. J. Am. Chem. Soc 141, 19817–19822 (2019). [PubMed: 31747522] Crystals of 3-substituted oxindole derivatives, which contain a new stereocenter at the γ carbon that were installed by the TrpB enzyme through directed-evolution, failed to generate structures by X-ray crystallography. MicroED achieved structure determination of several of these 3-substituted oxindole derivatives at supraresolution, allowing complete assignment of their stereocenters.

46. Qin J et al. Antitumor effects of brucine immuno-nanoparticles on hepatocellular carcinoma in vivo. Oncol. Lett 15, 6137–6146 (2018). [PubMed: 29731843]

47. Kutscher AH, Seguin L, Zegarelli EV & Piro JD Antimicrobial activity of thiostrepton: tube dilution studies. J. Am. Dent. Assoc 59, 715–720 (1959). [PubMed: 14412974]

48. Arrebola E, Cazorla FM, Perez-Garcia A & de Vicente A Chemical and metabolic aspects of antimetabolite toxins produced by Pseudomonas syringae pathovars. Toxins (Basel). 3, 1089–1110 (2011). [PubMed: 22069758]

49. Anderson B, Hodgkin DC & Viswamitra MA The structure of thiostrepton. Nature 225, 233–235 (1970). [PubMed: 5409975]

50. Martynowycz MW et al. Collection of Continuous Rotation MicroED Data from Ion Beam-Milled Crystals of Any Size. Structure 27, 545–548 (2019). [PubMed: 30661853]

51. Duyvesteyn HME et al. Machining protein microcrystals for structure determination by electron diffraction. Proc. Natl. Acad. Sci. U. S. A 115, 9569–9573 (2018). [PubMed: 30171169]

*52. Martynowycz MW, Zhao W, Hattne J, Jensen GJ & Gonen T Qualitative Analyses of Polishing and Precoating FIB Milled Crystals for MicroED. Structure 27, 1594–1600.e2 (2019). [PubMed: 31422911] FIB milling has been establishes as a tool to expand MicroED for structure determination of large crystals. Here, these studies applied an additional step called “polishing” to improve the MicroED diffraction quality of crystals from FIB milling.

53. Li X, Zhang S, Zhang J & Sun F In situ protein micro-crystal fabrication by cryo-FIB for electron diffraction. Biophys. Reports A, 339–347 (2018).

54. Zhou H, Luo Z & Li X Using focus ion beam to prepare crystal lamella for electron diffraction. J. Struct. Biol 205, 59–64 (2019). [PubMed: 30794865]

55. Carugo O & Carugo KD When X-rays modify the protein structure: Radiation damage at work. Trends Biochem. Sci 30, 213–219 (2005). [PubMed: 15817398]

56. Baker LA & Rubinstein JL Radiation damage in electron cryomicroscopy. Methods in Enzymology 481, (Elsevier Masson SAS, 2010).

57. Kmetko J, Husseini NS, Naides M, Kalinin Y & Thorne RE Quantifying X-ray radiation damage in protein crystals at cryogenic temperatures. Acta Crystallogr. Sect. D Biol. Crystallogr 62, 1030–1038 (2006). [PubMed: 16929104]

58. Ravelli RBG, Theveneau P, McSweeney S & Caffrey M Unit-cell volume change as a metric of radiation damage in crystals of macromolecules. J. Synchrotron Radiat 9, 355–360 (2002). [PubMed: 12409622]

59. Weik M et al. Specific chemical and structural damage to proteins produced by synchrotron radiation. Proc. Natl. Acad. Sci. U. S. A 97, 623–628 (2000). [PubMed: 10639129]

*60. Hattne J et al. Analysis of Global and Site-Specific Radiation Damage in Cryo-EM. Structure 26, 759–766.e4 (2018). [PubMed: 29706530] The first comprehensive study to decipher the effects of radiation damage during MicroED experiments with implications to all cryoEM studies. These studies found both global and site-specific radiation damage during MicroED studies.

61. Karuppasamy M, Karimi Nejadasl F, Vulovic M, Koster AJ & Ravelli RBG Radiation damage in single-particle cryo-electron microscopy: Effects of dose and dose rate. J. Synchrotron Radiat 18, 398–412 (2011). [PubMed: 21525648]

62. Wu S, Armache JP & Cheng Y Single-particle cryo-EM data acquisition by using direct electron detection camera. Reprod. Syst. Sex. Disord 65, 35–41 (2016).

**63. Hattne J, Martynowycz MW, Penczek PA & Gonen T MicroED with the Falcon III direct electron detector. IUCrJ, 6, 921–926 (2019).These studies applied the first usage of a FalconIII direct electron detector for mitigating radiation damage from MicroED studies. The use of the Falcon III detector collected data with higher completeness and lower radiation damage as compared to CMOS detectors.

**64. Martynowycz MW, Hattne J & Gonen T Experimental Phasing of MicroED Data Using Radiation Damage. Structure 28, 458–464.e2 (2020). [PubMed: 32023481] This study demonstrates the use of radiation damage for ab initio phasing with MicroED.

65. de la Cruz MJ, Martynowycz MW, Hattne J & Gonen T MicroED data collection with SerialEM. Ultramicroscopy 201, 77–80 (2019). [PubMed: 30986656]

66. Fernández-Busnadiego R et al. Insights into the molecular organization of the neuron by cryo-electron tomography. J. Electron Microsc. (Tokyo). 60, 137–148 (2011).

67. Bartesaghi A et al. 2.2 A resolution cryo-EM structure of β-galactosidase in complex with a cell-permeant inhibitor. Science (80-.). 348, 1147–1152 (2015).

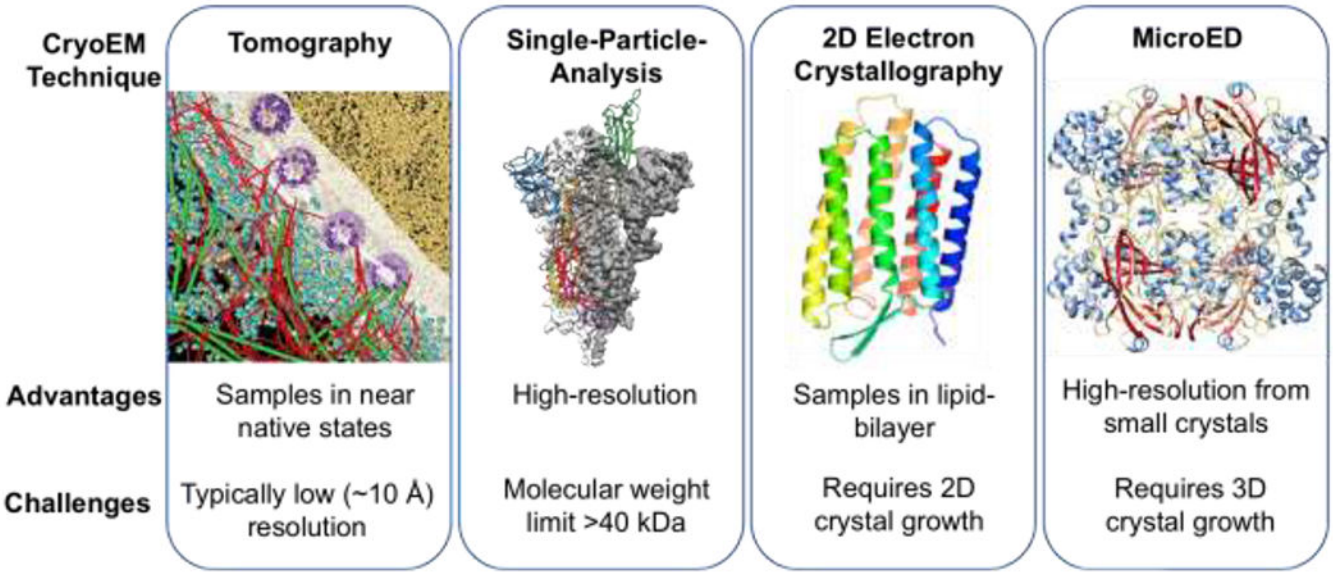

Figure 1. The four major modalities of cryoEM.

From left to right. A model of the HeLa cell nuclear periphery (Reprint from reference 24 with permission from AAAS) by tomography. Model of COVID-19 spike protein by SPA (Reprint from reference 25 with permission from AAAS). The structure of bacteriorhodopsin determined by electron crystallography (Reprint from reference 21) and the structure of catalase determined by MicroED (Reprint from reference 26).

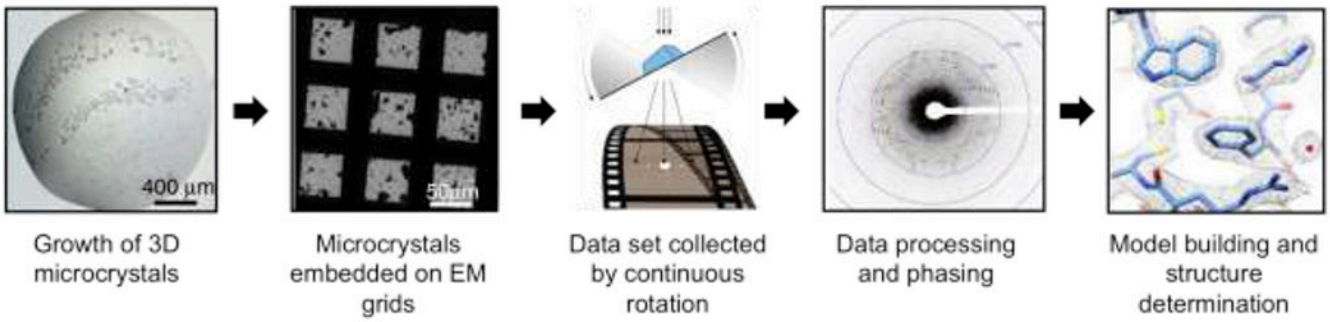

Figure 2. MicroED workflow.

From left to right. Crystals are grown, harvested, and placed directly on EM grids. Manual or automated screening to assess for electron diffraction of the crystals. When a well diffracting crystal is identified, a diffraction dataset is collected by continuous rotation. The diffraction dataset is then processed using standard crystallography software leading to model building and refinement.

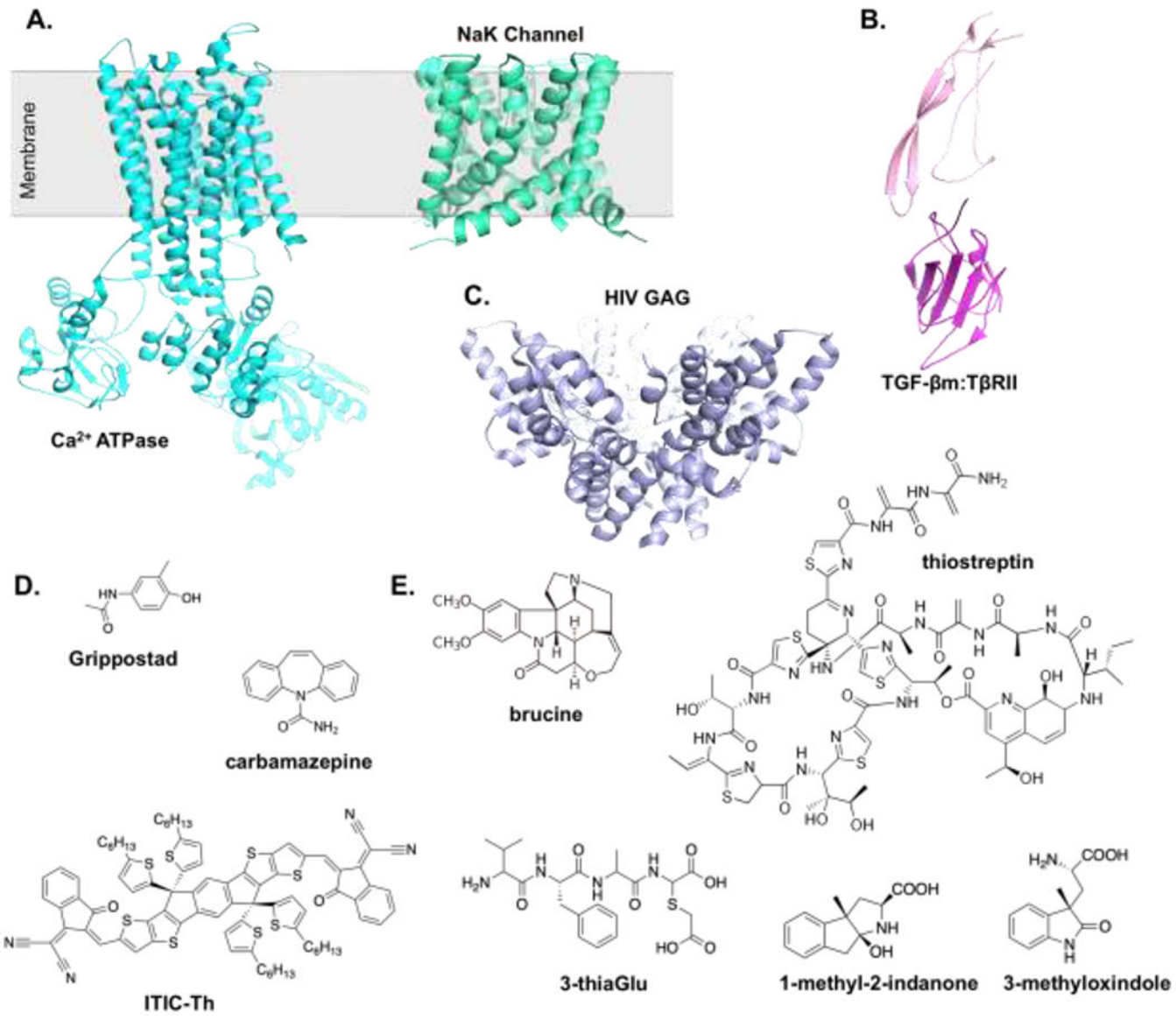

Figure 3. Representative MicroED structures of membrane proteins, protein complexes, small-molecules, and natural-products.

(A) MicroED structures of the membrane proteins rendered as cyan and green ribbon for Ca^{2+} ATPase (PDB 3J7T/U)[34] and NaK (PDB 6CPV)[35], repectively. **(B)** MircoED structure of the TGF-pm:TpRII protein-protein complex (PBD 5TY4)[36]. Protein rendered as pink and magenta ribbon for TGF-pm and TpRII, respectively. **(C)** MircoED structure of the HIV-GAG-bevirimat rendered as blue ribbon (PDB 6N3U)[39]. **(D)** A galley of small-molecules with structures determined by MircoED. **(E)** Examples of natural-products with structures determined by MircoED.

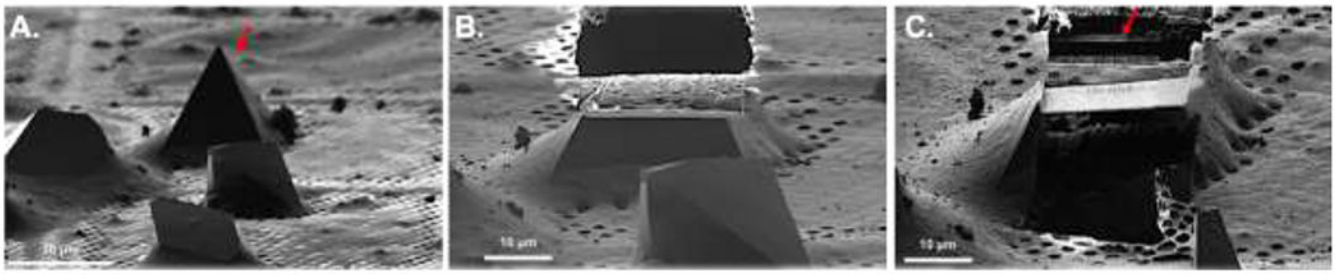

Figure 4. FIB milling of crystals for MicroED.

(A) Image of select proteinase K crystals at high magnification before milling. The arrow indicates the crystal that was milled in (C). (B) FIB image of select crystal from (A) after milling the top of the crystal. (C) FIB image of crystal after milling and cleaning both the top and bottom of the crystal leaving a lamella indicated by an arrow. (Reprint from reference 52).

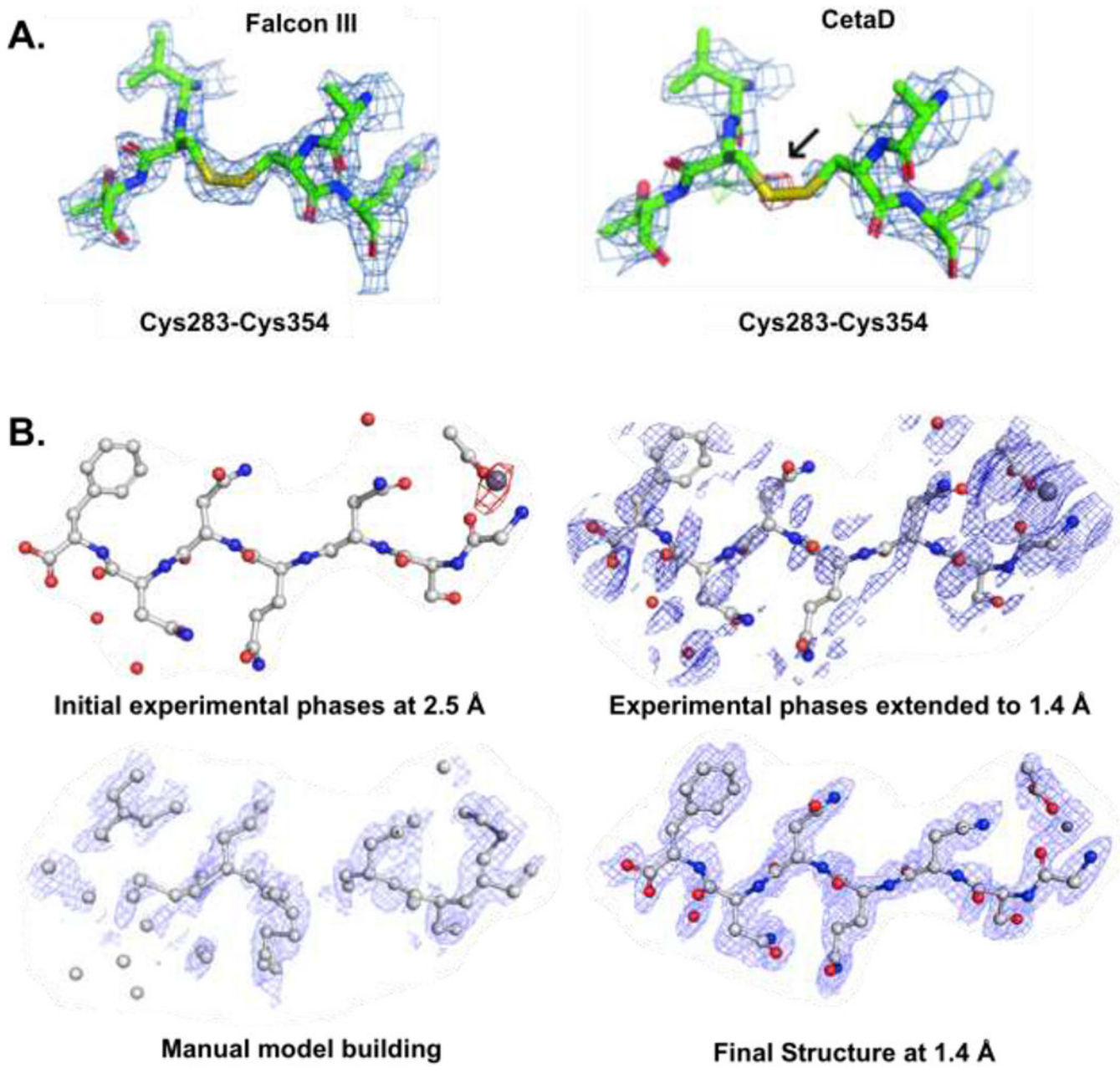

Figure 5. MicroED radiation damage and experimental phasing.

(A) Disulfide bonds of the proteinase K structures determined from data collected on Falcon III and CetaD. The density around the two disulfide bonds indicates increasing radiation damage as an effect of increasing dose. The positive difference density around Cβ of Cys283 in the CetaD data (black arrow) indicates a partially dislocated S atom. The 2mFo – DFc densities (blue meshes) are contoured at 1.5σ (Reprint of reference 63). **(B)** Fourier difference maps between the damaged and undamaged structure of the GSNQNNF peptide using the phases at 2.5-Å resolution, contoured at 3s (Top left). Maps of the experimental phases of the peptide extended to 1.4 Å (Top right). Maps of an intermediate model-building

step (Bottom left) to generate the final peptide structure at 1.4 Å (Bottom right). Reprint from reference 64.